

## Application of Walsh Transform to Interpret Residual Magnetic Anomalies due to Simple Geometrically Shaped Causative Targets

**Talal Ali Mokhtar**

*Department of Geophysics, Faculty of Earth Sciences,  
King Abdulaziz University,  
P.O. Box 80206, Jeddah 21589, Saudi Arabia  
tmokhtar@kau.edu.sa*

Received: 26/9/2006

Accepted: 25/3/2007

*Abstract.* A set of complete and orthogonal functions of nonsinusoidal waveform, known as Walsh functions which assume only discrete amplitude values of +1 and -1, are utilized for the analysis of magnetic data. Procedures are formulated using the Walsh transform for interpreting vertical magnetic anomalies of (1) the sphere (finite depth extent) (2) the horizontal circular cylinder, and (3) the vertical sheet of infinite depth extent. The applicability of the method has been tested on theoretical models. The method is also applied on the famous Kursk anomaly of a sheet of infinite depth extent, and the result is in good agreement with other published techniques.

*Keywords:* Walsh transform; Walsh spectra; sequency octave number; sphere; horizontal cylinder; vertical thin sheet; magnetic anomaly.

### **Introduction**

Isolated potential anomalies are quantitatively interpreted in terms of the location, depth, size, and shape of the causative source which constitutes an inverse problem in the potential field theory. The solution of such a problem is ambiguous and not complete either in theory or practice (Shaw and Agarwal, 1990). This ambiguity is further reinforced by uncertainties involving limited number

of observations and inappropriate separation of the regional and the residual anomalies from the observed field data. The approximation of causative sources by some simple geometrical shapes such as a sphere, a cylinder, a vertical thin sheet, a prism, *etc.*, or combination of these geometrical shapes are attempted to resemble the real geology (Shaw and Agarwal, 1990).

Spectral analysis has been extensively used in every field of the geophysical data processing and interpretation. Frequency-domain analysis has an advantage over the space-domain analysis due to existence of a clear relationship of various body parameters in the frequency-domain (Bhattacharyya and Leu, 1977, Shaw and Agarwal, 1990).

Since the magnetic field due to any dipole distribution is a periodic, which analogies to mass distribution in gravity field (Shaw and Agarwal, 1990), its spectral analysis involves domain transformation rather than its series decomposition into component functions. Frequency-domain has been extensively used during the last few decades that the Fourier transform (FT) has become almost synonymous with spectral analysis. In general, any transform whose kernel functions are a complete and orthogonal set can be utilized to decompose a function satisfying Dirichlet's conditions into its constituents (Shaw and Agarwal, 1990). There is a set of complete and orthogonal functions similar to sinusoidal functions but rectangular in waveform with amplitude either +1 and -1 and is known as Walsh functions (Walsh, 1923). Walsh functions constitute the kernel of the Walsh transform (WT). It is difficult to obtain the WT of a given signal in closed form since Walsh functions are discontinuous in their domain (Shaw and Agarwal, 1990). Therefore, the numerical solution can be obtained by additive manipulation of the discrete data sequences. The application of FT in potential field data interpretations (Dean, 1958; Odegard and Berg, 1965; Bhattacharyya and Leu, 1977), some publications on WT (Gubbins *et al.*, 1971; Lanning and Johnson, 1983), the application of Walsh transforms to interpret gravity anomalies due to simple geometrically shape sources (Shaw and Agarwal, 1990) and the density mapping from a gravity data using the Walsh transform (Keating, 1992) have encouraged me to examine the feasibility of WT to the problem of magnetic field.

This paper discusses the possible application of WT in interpretations of isolated vertical magnetic field data over a sphere, a horizontal cylinder and a vertical thin sheet of infinite extent. The magnetic fields due to these simple models are subjected to Walsh transforms for computing Walsh power spectra. Walsh spectra of these models are subjected to detailed and careful analyses for determining the causative body's parameters.

This analysis, is called as "sequency octave analysis" (SOA) after Shaw and Agarwal (1990), does not employ the whole spectrum for interpretation. It rather uses some representative spectral points. The distribution of the Walsh power spectrum in the sequency octave depends on the depth of causative sources. A scheme based on the empirical relationship between depth and sequency has been implemented to estimate the depth to the causative body.

### Theory

Figure 1 shows the first ten Walsh functions and their corresponding sinusoids functions for comparison. The concept of frequency ( $f$ ) as the reciprocal of time period ( $T$ ) for periodic function does not apply to Walsh functions because they may not be periodic (Shaw and Agarwal, 1990). The sequency or generalized frequency, is a term that has been proposed by Harmuth (1972) to describe a periodic repetition rate that is independent of the waveform and is defined as one half of the average number of zero crossing per unit time interval. Therefore, the sequency and frequency are the same for periodic functions. However, for functions not truly periodic sequency is a measure of average periodicity.

The set of Walsh functions can be generated from a difference equation which uses lower order sequency functions to develop higher order ones (Beauchamp, 1975, p. 21). Sequency order is preferable for communications and signal processing such as spectral analysis and filtering (Beauchamp, 1975). This is needed to identify some pattern in the amplitude and power spectra of the WT of magnetic anomaly to determine the causative body parameters.

Walsh functions of higher orders can be found by higher orders from

$$\begin{aligned} \text{WAL}(2m + q, t) &= (-1)^{[m/2]+q} [\text{WAL}(m, 2t) + (-1)^{m+q} \text{WAL}(m, 2(t-1/2))] \quad (1) \\ & \qquad \qquad \qquad \text{for } 0 \leq t \leq 1 \\ & = 0 \qquad \qquad \qquad 0 > t > 1 \end{aligned}$$

with  $\text{WAL}(0, t) = 1, 0 \leq t \leq 1$ , where  $q = 0$  or  $1$  and  $m = 0, 1, 2, \dots$  represents the sequency order of the Walsh functions.  $[m/2]$  means the largest integer smaller or equal to  $m/2$  (Beauchamp, 1975). Figure 1 shows that even numbered Walsh functions are symmetric and odd numbered ones are antisymmetric with respect to the midpoint of the interval  $(0, 1)$ . This behavior is analogous to the relationship of cosine and sine functions, as introduced by Harmuth (1972) as

$$\begin{aligned} \text{WAL}(2m, t) &= \text{CAL}(m, t) \\ \text{WAL}(2m - 1, t) &= \text{SAL}(m, t) \quad (2) \\ m &= 0, 1, \dots, N/2 \end{aligned}$$

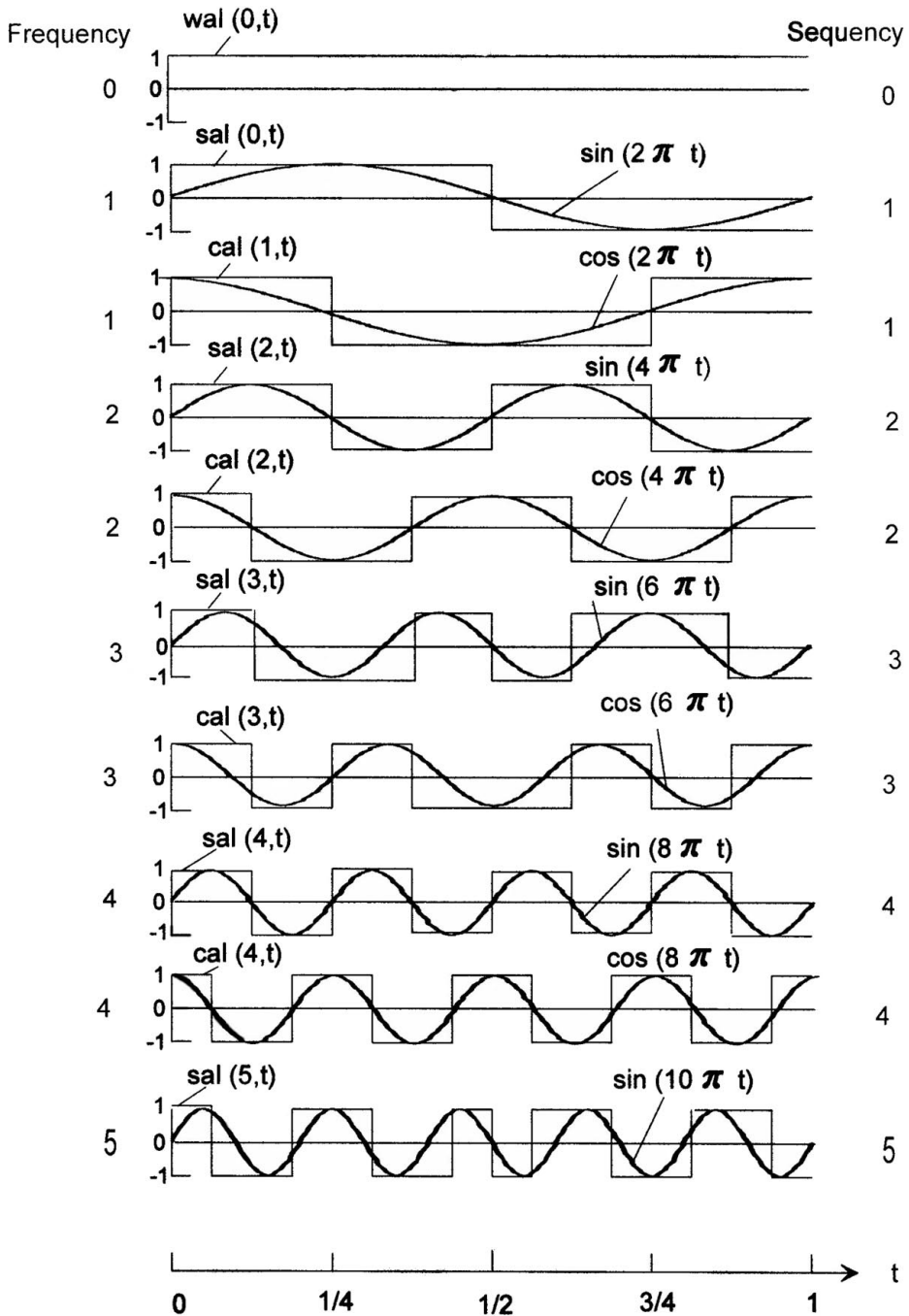


Fig. 1. The first ten sequency Walsh functions with their equivalent Fourier harmonics.

Every function  $f(t)$  that is integrable in the Lebesgue sense can be presented by an infinite series of Walsh functions over the interval  $[0, 1]$  (Beauchamp, 1975, p. 40). The WT pair is defined as

$$f(t) = \sum_{m=0}^{\infty} F(m) \text{ WAL}(m, t) \quad (3a)$$

$$F(m) = \int_0^1 f(t) \text{ WAL}(m, t) dt, \quad \text{for } m = 0, 1, 2, \dots \quad (3b)$$

The integration shown in equation (3b) can be replaced by summation using the trapezium rule on  $N$  ( $N$  evenly spaced  $= 2^n$ ,  $n$  being a positive integer) sampling points  $\{x(i)\}$  and then the finite discrete Walsh transform (DWT) can be written as

$$X(m) = \frac{1}{N} \sum_{i=0}^{N-1} x(i) \text{ WAL}(m, i), \quad m = 0, 1, 2, \dots, N-1 \quad (4a)$$

$$x(i) = \sum_{m=0}^{N-1} X(m) \text{ WAL}(m, i), \quad m = 0, 1, 2, \dots, N-1 \quad (4b)$$

The Walsh power spectrum  $P(m)$  for the signal of finite data point  $\{x(i)\}$  can be obtained as (Beauchamp, 1975, p. 100)

$$P(0) = X_c^2(0),$$

$$P(m) = X_c^2(m) + X_s^2(m), \quad m = 1, 2, \dots, N/2 - 1. \quad (5)$$

$$P(N/2) = X_s^2(N/2)$$

Thus, the WT of  $N$  point signal contains  $(N/2) + 1$  spectral points.

### ***Comparison of Walsh and Fourier Transform Properties***

A comparison of Walsh and Fourier transform properties had been discussed and summarized by Show and Agarwal (1990) and Beauchamp (1975, p. 72). The relevant propositions to this work can be listed below.

*Stability of power spectra:* Walsh power spectra are invariant under dayatic, and not cyclic, shifts whereas Fourier power spectra are invariant under cyclic (linear) shifts of data sequences. However, it has been observed that a small translational shift in the data with respect to a fixed origin generates practically insignificant effects on the Walsh power spectra based on equation (5) Beauchamp (1975, p. 45, 89).

*Time-domain properties:* Convolution, correlation, etc., cannot be implemented as in the Fourier transform in the frequency-domain without any linear time-shift properties of Walsh transform in the sequency domain. However, assuming dyatic time delay instead of a linear one, convolution and correlation would have the same mathematical form in sequency domain as in the frequency-domain. More work is needed to assess the advantage of the WT in identifying such properties as earth signal with no noise (Shaw and Agarwal, 1990).

*Computational efficiency:* The computation of WT of  $N(= 2^n, n$  is a positive integer) real data using fast WT subroutine can be obtained from  $N \times n$  simple additions without involving any multiplication operation whereas through the fast FT subroutine, the FT of the same signal requires  $N \times n$  complex multiplications and evaluation of  $N/2$  complex exponentials (Shaw and Agarwal, 1990).

*Filtering operations:* Bath (1974, p. 116) noticed that for digital filtering, the "Walsh transform is superior in having no Gibbs phenomenon and not requiring any special windowing in time-domain" comparing to FT. Beauchamp (1975, p. 173) and Shaw and Agarwal (1990) stated that "The results of WT are obtained in one-eighth of the computational time of the FT calculations and give almost the same information" for a matched filtering example.

## Formulation of Problem

Formulation of the problem is utilizing the technique that was proposed by (Shaw and Agarwal, 1990). The main objective of this paper is to examine the capability of using the Walsh transform as a technique in magnetic data interpretation to estimate the causative sources parameters. To implement this objective, there are two steps: (a) Computation of the Walsh power spectra of magnetic fields over a few simple geometrically shaped causative sources, such as, a sphere, a horizontal cylinder and a vertical thin sheet, with known body parameters and then developing interpretation schemes using some pattern(s) of the spectra. This represents a forward problem. A sphere, a horizontal cylinder and a vertical thin sheet are considered that their magnetic fields are given by simple mathematical equations. (b) a suitable field data is analyzed by the developed scheme for the interpretation.

### *Sequency Octave Analysis*

Figure 2 shows the Walsh power spectra of vertical magnetic anomalies over a sphere, a horizontal cylinder and a vertical thin sheet. The distribution of Walsh power spectra of vertical magnetic fields over the sphere and the horizontal cylinder exhibits similar patterns which are different from that for the

vertical thin sheet. It has been observed that the maximum Walsh power spectra shifts to the lower sequency number as the depth of the causative body increasing. This maybe attributed to the low frequency wavelength content of an anomaly increases with depth. Therefore, a lower sequency number implies a longer Walsh base function and this equivalent to a longer wavelength. It has been also noticed that the distribution of Walsh power spectrum over a vertical thin sheet, in magnetic case, shows generally the same pattern as shown over the sphere and the 2-D horizontal cylinder in the gravity case (Shaw and Agarwal, 1990), because the magnetic field over the vertical thin sheet model resembles line of monopoles (Sharma, 1997, p. 88). The causative body parameters cannot be interpreted by considering the whole power spectrum as a result of the random behavior of the spectrum (Shaw and Agarwal, 1990).

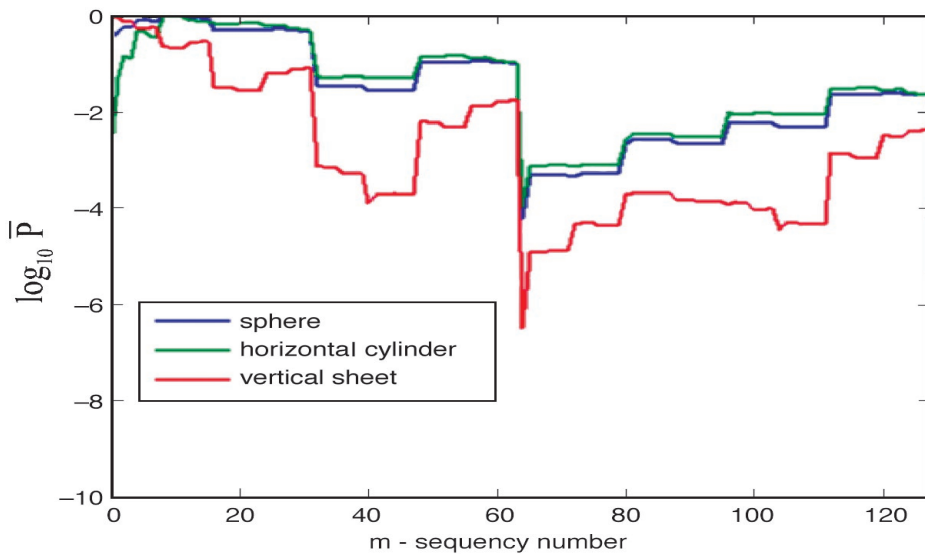


**Fig. 2.** Walsh power spectrum of residual anomaly of the vertical magnetic field due to a sphere, a horizontal circular cylinder and a vertical sheet of infinite extent of radius = 1 units, depth = 5 units and magnetic susceptibility contrast = 1 units. Values are in arbitrary units.

It has been observed specially in vertical thin sheet case that the spectral peaks at a certain sequences  $Q_j (=2^j - 1, j = 0, 1, 2, \dots, n - 1)$ , which have been also termed after Shaw and Agarwal (1990) as "sequency octave number" when peak spectral power from each group is considered. Figures 5, 6 and 7 show the power distribution of the spectral points  $Q_j$  which are related to the depth of the causative sources. The analysis utilizes spectral power separated repeatedly by one octave as  $2^{j-1}$  points on the sequency axis. Shaw and Agarwal (1990) termed this process as "sequency octave analysis" (SOA).

Figures 3, 4 and 5 show the sequency octave power spectra of the magnetic fields over the sphere, the horizontal cylinder and the vertical thin sheet, respectively. It can be seen from these figures that the sequency octave power spectra exhibits more flatness of the octave spectra as the depth decreased. Thus, SOA depends on the horizontal gradient of the signal.

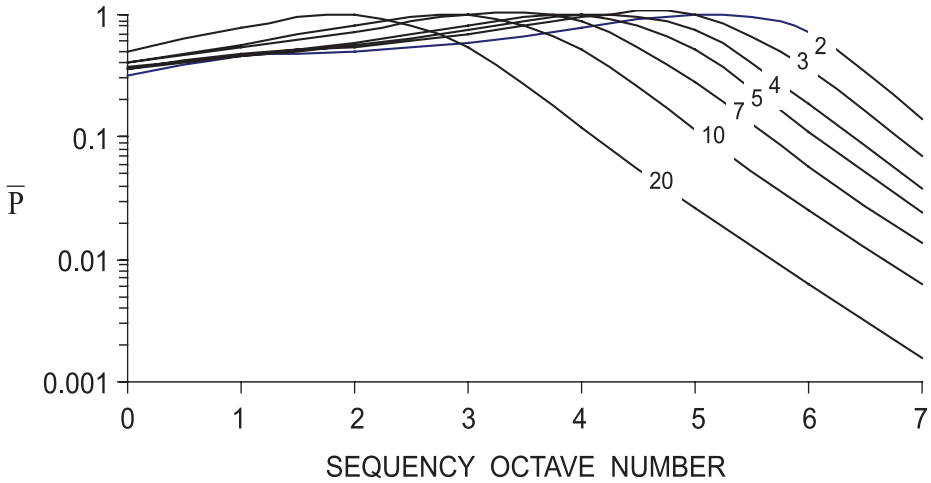


Fig. 3. Sequency octave power spectra of magnetic anomalies due to a sphere (dipole) for indicated depth values.

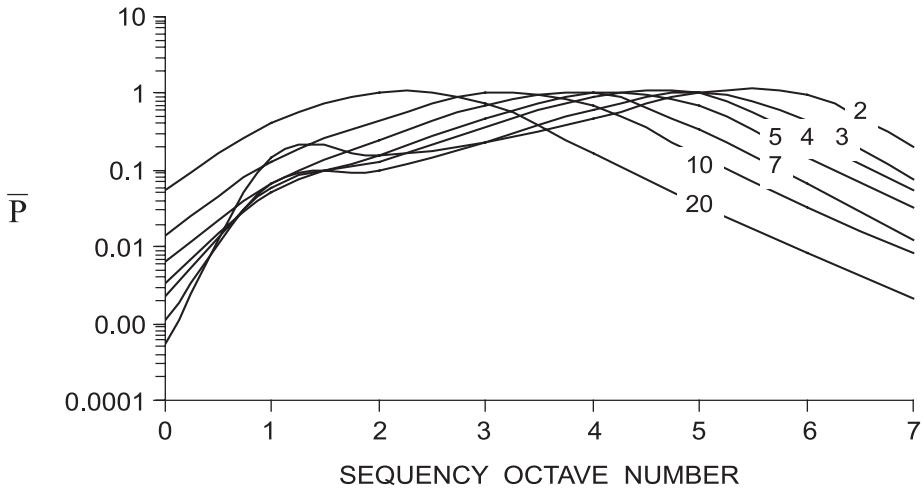


Fig. 4. Sequency octave power spectra of magnetic anomalies due to a 2-D horizontal cylinder (dipole) for indicated depth values.



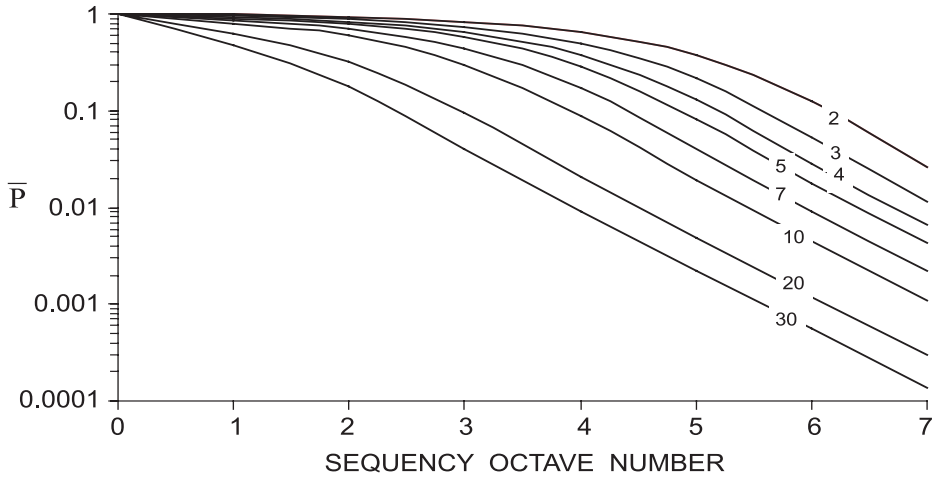


Fig. 5. Sequency octave spectra of gravity anomalies due to a thin vertical sheet for indicated depth values.

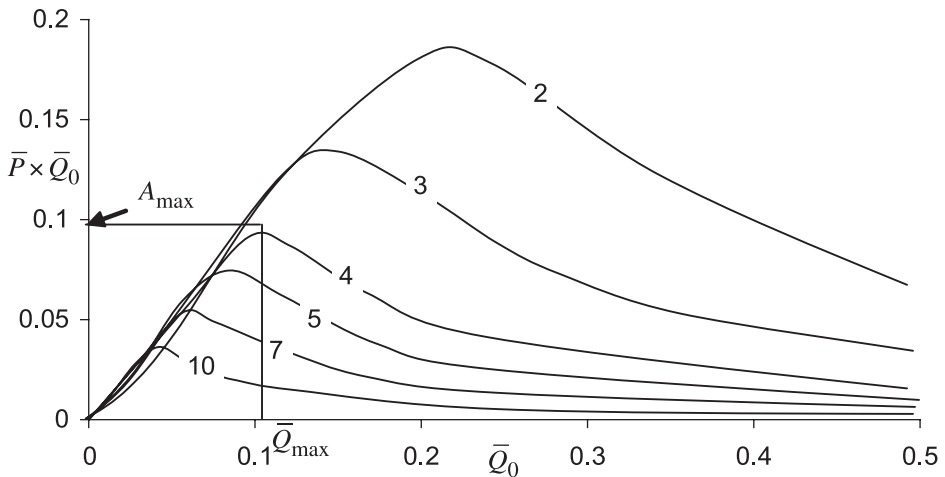


Fig. 6. Plot of  $\bar{P} \times \bar{Q}_0$  versus normalized octave sequency  $\bar{Q}_0$  for a spherical causative body showing the dependence of the peak position  $\bar{Q}_{max}$  on depth as indicated on the curves.

### Interpretation Scheme

The observed signal is Walsh transformed and analyzed using SOA. Then, the pattern using SOA is correlated with the body parameter of the source. The sequency octave power spectrum shows a dependence on the data length and hence cannot be used directly for depth estimation. This difficulty has been solved by normalizing the sequency with profile length. This is done by fixing the domain of normalized octave sequency ( $\bar{Q}_0 = Q_j/N$ ) between 0 and 1/2.

The plots of spectral value  $\bar{P}(= P/P_{\max}) \times \bar{Q}_0$  versus  $\bar{Q}_0$  for the spheres targets of different depths, shown in Fig. 6, exhibit peaks at certain normalized octave sequencies  $\bar{Q}_{\max}$ . The value of  $\bar{Q}_{\max}$  in this figure is govern by the depth to the sphere. An empirical equation

$$\bar{Q}_{\max} \times \text{depth} = 0.45 \tag{6}$$

has been computed for depth determination. A similar equation for horizontal cylinder is given by

$$\bar{Q}_{\max} \times \text{depth} = 0.50 \tag{7}$$

has been computed for depth determination.

For a vertical thin sheet model, a plot of the spectral  $\log_2 \bar{P} \times \log_2 \bar{Q}_0$  versus  $\bar{Q}_0$  for different depths is shown in Fig. 7, which reveals peaks at certain normalized octave sequencies  $\bar{Q}_{\max}$ . An empirical equation

$$\text{depth} = (-\ln \bar{Q}_{\max} - 0.559) / \bar{Q}_{\max} \tag{8}$$

has been computed for depth determination.

The interpretation scheme based on the empirical equations for analyzing field data is illustrated in Fig. 8.

To evaluate the applicability of any transformed domain such as this problem, I have examined carefully the effects of profile length and sampling interval. These effects on the Walsh power spectrum by numerical computation.

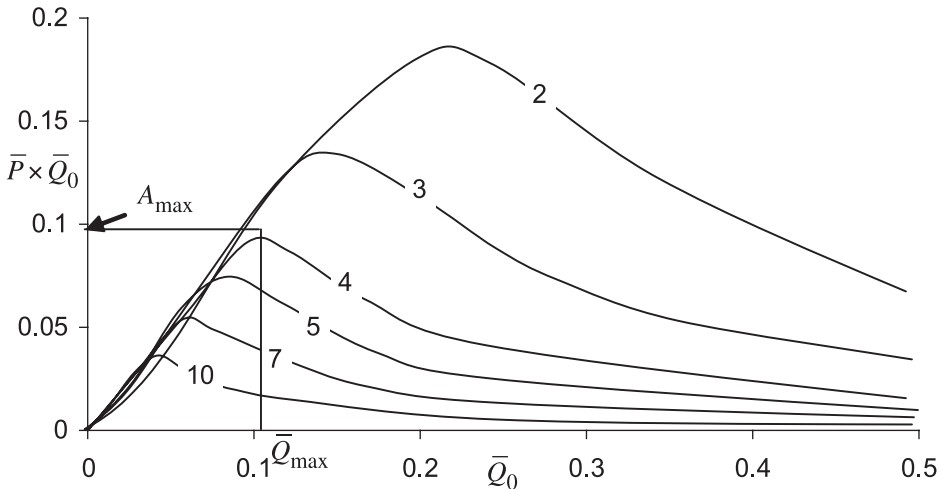


Fig. 7. Plot of  $\log_2 \bar{P} \times \log_2 \bar{Q}_0$  versus  $\bar{Q}_0$  for a thin vertical sheet of infinite depth extent for indicated depth values, showing the change in peak positions.

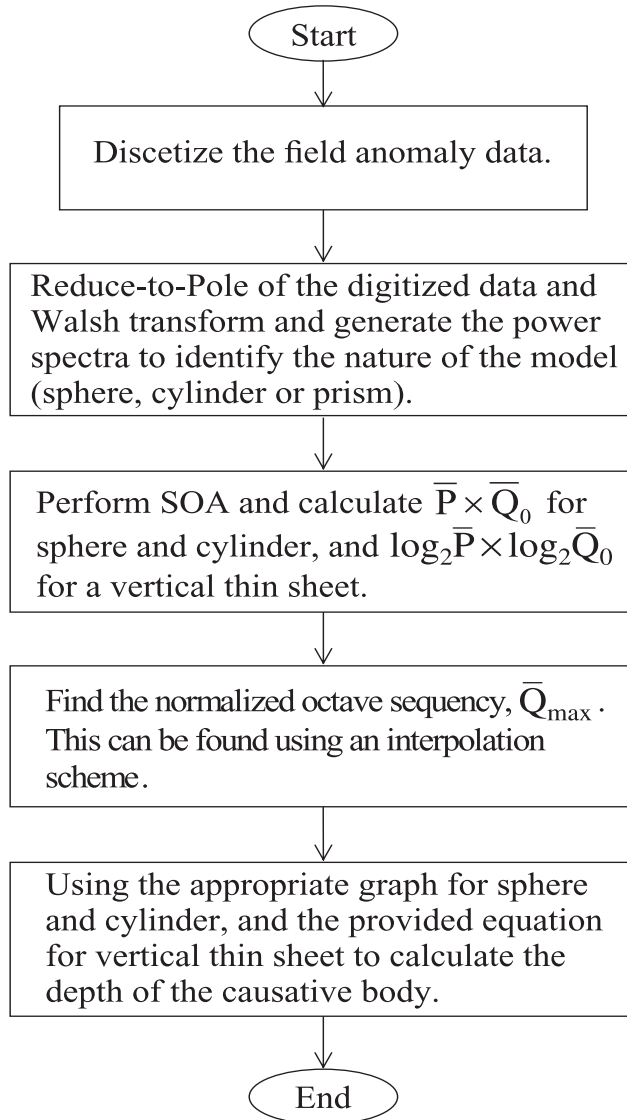


Fig. 8. Flow chart a generalized approach for depth estimation.

### ***Effect of Profile Length***

The computed values of the product of normalized Walsh power spectra  $\bar{P}$  and normalized octave sequency  $\bar{Q}_0$  with octave number  $j$  for profile length varying from 512 to 64 data points considering vertical thin sheet causative source at a depth of five unites are shown in Table 1. The maximum amplitude

$A_{\max}$  of  $\log_2 \bar{P} \times \log_2 \bar{Q}_0$  and its corresponding normalized octave sequency  $\bar{Q}_{\max}$  are also tabulated. It is obvious from the table that a profile length of 25.6 times the depth value is enough to estimate the depth via SOA of the Walsh power spectra.

**Table 1. Effect of profile length on sequency octave analysis for a vertical thin sheet at a depth of five units.**

| Sequency octave number | $\log_2 \bar{P} \times \log_2 \bar{Q}_0$ with unit sampling interval and profile length of |         |         |          |
|------------------------|--|---------|---------|----------|
|                        | 512  | 256     | 128     | 64       |
| 0                      | –  | –       | –       | –        |
| 1                      | 0.60653  | 1.14643 | 2.13701 | 3.96379  |
| 2                      | 1.24298  | 2.26554 | 4.08413 | 7.13812  |
| 3                      | 2.36767  | 4.21694 | 7.24192 | 10.77973 |
| 4                      | 4.30447  | 7.33836 | 10.8421 | 11.54810 |
| 5                      | 7.39905  | 10.9049 | 11.6184 | 7.71650  |
| 6                      | 10.9445  | 11.6750 | 7.81749 | –        |
| 7                      | 11.7090  | 7.87861 | –       | –        |
| 8                      | 7.91216  | –       | –       | –        |
| $A_{\max}$             | 11.95  | 11.9    | 11.8    | 11.7     |
| $\bar{Q}_{\max}$       | 0.205  | 0.205   | 0.204   | 0.201    |
| Computed depth         | 5.003  | 5.003   | 5.05    | 5.201    |
| Actual depth           | 5.000  | 5.000   | 5.000   | 5.000    |

### ***Effect of Sampling Interval***

The computation for the same model for a fixed profile length of 512 units with sampling interval equals to 1, 2 and 4 units are shown in Table 2. It is evident from this table that for different sampling intervals, the value of  $\bar{Q}_{\max}$  changes and the correct value of depth is obtain from equation (8) in the three cases.

### **Field Example**

The validity of the above procedure is demonstrated by the analysis of the well-known Kurks anomaly (Fig. 9) (Werner, 1953 and Mohen *et al.*, 1982). The anomaly has been digitized at an interval of 23.4375 m. The discrete data then have been subjected to Walsh transform and SOA. The Walsh power spectral patterns are shown in Fig. 10. The patterns are closely resembling the pattern due vertical thin sheet of infinite depth extent. The product of  $\log_2 \bar{P} \times$

**Table 2. Effect of sample interval on sequency octave analysis for a vertical thin sheet at a depth of five units.**

| Sequency octave number | $\log_2 \bar{P} \times \log_2 \bar{Q}_0$ for a fixed profile length of 512 units with sampling interval of |          |          |
|------------------------|--|----------|----------|
|                        | 1  | 2        | 3        |
| 0                      | –  | –        | –        |
| 1                      | 0.60653  | 0.390106 | 0.322175 |
| 2                      | 1.24298  | 0.948763 | 0.782793 |
| 3                      | 2.36767  | 1.874387 | 1.493266 |
| 4                      | 4.30447  | 3.366806 | 2.507065 |
| 5                      | 7.39905  | 5.54117  | 3.62237  |
| 6                      | 10.9445  | 7.39602  | 3.561439 |
| 7                      | 11.7090  | 5.912035 | –        |
| 8                      | 7.91216  | –        | –        |
| $A_{\max}$             | 11.95  | 7.4      | 3.7      |
| $Q_{\max}$             | 0.205  | 0.28     | 0.36     |
| Computed depth         | 5.003  | 5.09     | 5.14     |
| Actual depth           | 5.000  | 5.000    | 5.000    |

$\log_2 \bar{Q}_0$  versus  $\bar{Q}_0$  is shown in Fig. 11. The depth estimate to the top of the causative body, using Equation (8), is 304.93 m by the Walsh transform which agreed with the results obtained by Mohen *et al.* (1982) and Werner (1953) (Table 3).

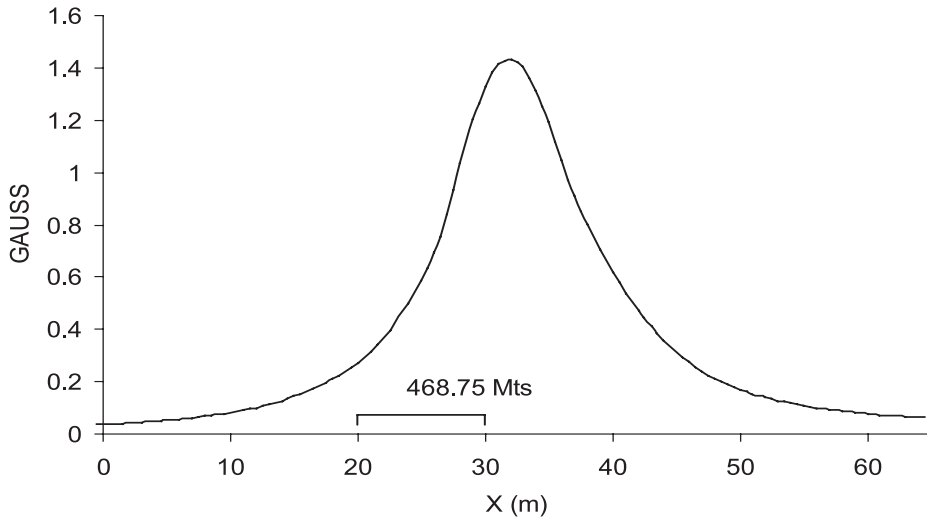


**Fig. 9. The Kursk field anomaly.**

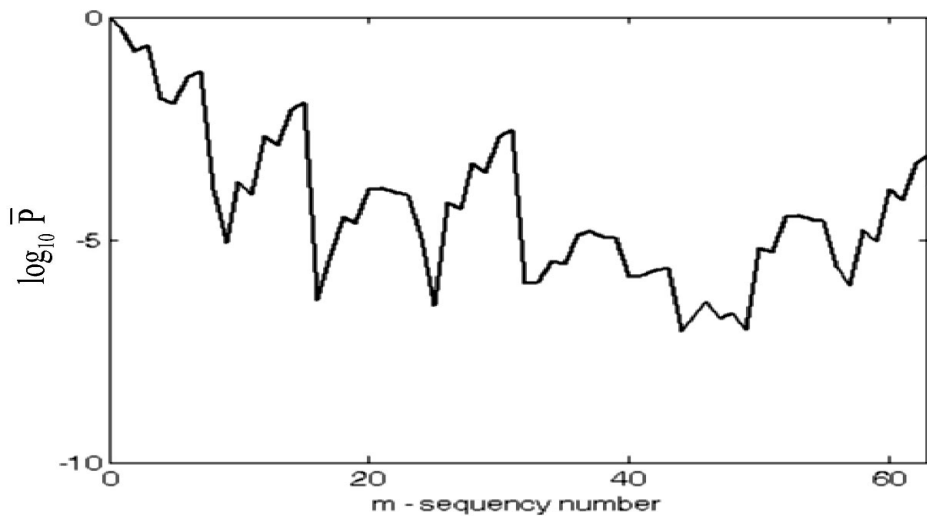


Fig. 10. Walsh power spectrum of Kursk anomaly.

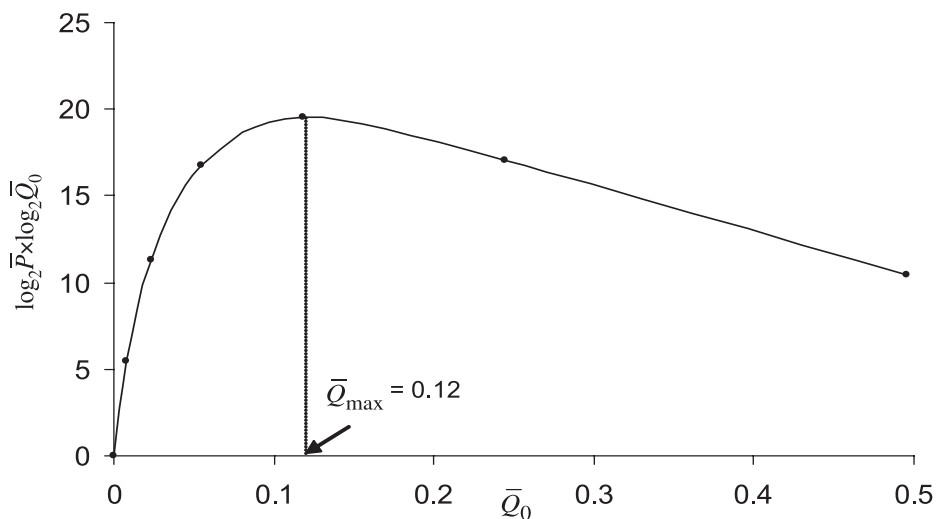


Fig. 11. Plot  $\log_2 \bar{P} \times \log_2 \bar{Q}_0$  versus normalized octave frequency  $\bar{Q}_0$  for the Kursk anomaly.

Table 3. Comparison between depth estimated from the present technique and other authors.

| Parameter | Method        |                            |                            |                           |                   |
|-----------|---------------|----------------------------|----------------------------|---------------------------|-------------------|
|           | Werner (1953) | Mohen <i>et al.</i> (1982) | Mohen <i>et al.</i> (1990) | Kara <i>et al.</i> (1998) | Present technique |
| Depth (m) | 282           | 304.69                     | 301.22                     | 291.00                    | 304.93            |

## Conclusions and Discussions

It was shown that, the Walsh transforms can be used for interpretation of magnetic anomalies caused by bodies of some simple geometrically shapes such as a sphere, a horizontal cylinder and vertical thin sheet. The Walsh power spectra of magnetic fields due to assumed sources show a noticeable variations which have been used to identify the shape of causative body. A methodology for interpretation to estimate depth parameters based on the SOA is developed which is independent of the data length of the field signal. The ratio of depth to the data spacing is very important in the potential field data; therefore, the effect of data interval shows insignificantly affecting the accuracy which can be assumed relatively to the depth as 2 without affecting the accuracy of depth estimation. The analysis of the field data of Kursk magnetic anomaly demonstrated the applicability of this technique.

### *Acknowledgment*

The author is thankful to Dr. Zaki Sen, of Saudi Arabian Geological Survey, and Dr. Ahmed Balaamash, of electrical engineering, King Abdulaziz University for discussions in the beginning of this work. The author also wishes to record his sincere thanks to Dr. Mansour Al-Garni for his lengthy valuable discussions. The author is also thankful to the Department of Geophysics for providing necessary facilities to implement this work.

### References

- Ahmed, N. and Rao, K.R.** (1975) *Orthogonal Transforms for Digital Signal Processing*, New York: Springer-Verlag, Inc.
- Beauchamp, K.G.** (1975) *Walsh Functions and Their Applications*, Academic Press Inc.
- Bhattacharya, B.K. and Leu, L.K.** (1977) Spectral analysis of gravity and magnetic anomalies due to rectangular prismatic bodies, *Geophysics*, **42**: 41-50.
- Dean, W.C.** (1985) Frequency analysis for gravity and magnetic interpretation, *Geophysics*, **23**: 41-50.
- Gubbins, D., Scollar, I. and Wisskirchen, P.** (1971) Two Dimensional Digital Filtering with Haar and Walsh transforms, *Ann. Geophys.*, **27**: 85-104.
- Gay, S.P. Jr.** (1963) Standard curves for interpretation of magnetic anomalies over long tabular bodies, *Geophysics*, **28**: 161-200.
- Gay, S.P. Jr.** (1965) Standard curves for interpretation of magnetic anomalies over long horizontal cylinders, *Geophysics*, **30**: 818-828.
- Harmuth, H.F.** (1972) *Transmission of Information by Orthogonal Functions*, New York, Springer-Verlag, Inc.
- Keating, P.** (1992) Density mapping from gravity data using Walsh transform, *Geophysics*, **57**: 637-1642.
- Lanning, E.N. and Johnson, D.M.** (1983) Automated identification of rock boundaries: An application of Walsh transform to geophysical well-log analysis, *Geophysics*, **48**: 197-205.

- Mohen N.L., Sundararajan N. and Seshagiri Rao, S.V.** (1982) Interpretation of some two-dimensional magnetic bodies using Hilbert transforms, *Geophysics*, **47**: 376-387.
- Odegard, M.E. and Berg, J.W.** (1965) Gravity interpretation using the Fourier integral, *Geophysics*, **30**: 424-438.
- Prakasa Rao, T.K.S. and Krishna Murthy, A.S.** (1986) A direct method of interpreting magnetic anomalies caused by long horizontal cylinders, *Boll. Geofis. Teor. Ed. Appl.*, **XIX**: 72-76.
- Sharma, P.V.** (1997) *Environmental and Engineering Geophysics*, Cambridge University Press.
- Shaw, R.k. And Agarwal, B.n. P.** (1990) The Application Of Walsh Transforms To Interpret Gravity anomalies due to some simple geometrically shaped causative sources: A feasibility study, *Geophysics*, **55**: 843-850.
- Walsh, J.L.** (1923) A closed set of orthogonal functions, *Am. J. Math.*, **45**: 5-24.
- Werner, S.** (1953) Interpretation of magnetic anomalies at sheet-like bodies, *Sveriges Geologiska Undersokning, Serie C*, N. 508. Stockholm.



## تطبيق تحويل والش لتفسير الشاذات المغنطيسية الناجمة من أشكال هندسية بسيطة

طلال علي مختار

قسم الجيوفيزياء، كلية علوم الأرض، جامعة الملك عبد العزيز  
ص.ب. ٨٠٢٠٦، جدة ٢١٥٨٩، المملكة العربية السعودية  
tmokhtar@kau.edu.sa

المستخلص. تعرف مجموعة الوظائف الكاملة والمتعامدة لشكل الموجة غير الجيبية بوظائف والش حيث تتراوح قيم المدى غير المتصل بين  $1+$  و  $1-$ ، والتي تستخدم في تحليل البيانات المغنطيسية، الإجراءات تم صياغتها باستخدام تحويل والش لتفسير الشاذات المغنطيسية العمودية ل: (١) كرة (ذات عمق محدود)، (٢) أسطوانة دائرية أفقية، و (٣) صفيحة عمودية غير محدودة العمق. وتم اختبار تطبيقات على نماذج رياضية. وكذلك طبقت الطريقة على شاذة كورسكا المغنطيسية المعروفة كصفيحة غير محدودة العمق وقد اتفقت النتائج مع نتائج التقنيات الأخرى المنشورة لنفس الشاذة.